Traffic 2007; **8:** 1521–1529
Blackwell Munksgaard

© 2007 The Authors
Journal compilation © 2007 Blackwell Publishing Ltd

doi: 10.1111/j.1600-0854.2007.00638.x

Migration Cues Induce Chromatin Alterations

Gabi Gerlitz[1,2], Idit Livnat[1], Carmit Ziv[3], Oded Yarden[3], Michael Bustin[2,*] and Orly Reiner[1,*]

[1]*The Department of Molecular Genetics, The Weizmann Institute of Science, Rehovot 76100, Israel*
[2]*Protein Section, Laboratory of Metabolism, National Cancer Institute, US National Institutes of Health, Bethesda, MD 20892, USA*
[3]*The Department of Plant Pathology and Microbiology, The Faculty of Agricultural, Food and Environmental Quality Sciences, The Hebrew University of Jerusalem, Rehovot 76100, Israel*
**Corresponding author: Orly Reiner, orly.reiner@weizmann.ac.il or Michael Bustin, bustin@helix.nih.gov*

Directed cell migration is a property central to multiple basic biological processes. Here, we show that directed cell migration is associated with global changes in the chromatin fiber. Polarized posttranslational changes in histone H1 along with a transient decrease in H1 mobility were detected in cells facing the scratch in a wound healing assay. In parallel to the changes in H1, the levels of the heterochromatin marker histone H3 lysine 9 tri-methylation were elevated. Interestingly, reduction of the chromatin-binding affinity of H1 altered the cell migration rates. Moreover, migration-associated changes in histone H1 were observed during nuclear motility in the simple multicellular organism *Neurospora crassa*. Our studies suggest that dynamic reorganization of the chromatin fiber is an early event in the cellular response to migration cues.

Key words: chromatin, histone H1, histone modifications, migration

Received 15 March 2007, revised and accepted for publication 8 August 2007, uncorrected manuscript published online 10 August 2007, published online 6 September 2007

Directed cell migration is a fundamental property of both simple and complex organisms, which is necessary for the proper execution of various biological processes including foraging, embryonic development, immunity, tissue repair and homeostasis. Improper cell migration is an underlying cause of numerous pathological conditions such as vascular diseases, chronic inflammatory diseases, cancer and cognitive disorders. Induction of directed cell migration results in cellular polarization, a process that involves dynamic changes in the actin cytoskeleton and in the adhesion molecules. In parallel, the microtubule-organizing center and the Golgi apparatus are reoriented (1,2) through nuclear movement (3). The nuclei of migrating cells display a wide range of structural changes. Developmentally related nuclear polarization has been noted in the single cell algae *Chlamydomonas*, where nuclear pore complexes localize to the posterior side of the nucleus and heterochromatin to the anterior side of the nucleus (4). Cancer cells change their nuclear shape and assume an elongated structure in capillaries (5). Migrating neurons change the structure of the nucleus during migration in a prototypic fashion (6,7). These types of morphological changes of the cell nucleus raise the possibility that cell migration is associated with the reorganization of the chromatin fiber. This possibility, which has obvious functional consequences, has not been investigated in detail yet.

To monitor possible chromatin structural changes, we focused on histone H1, one of the most abundant and ubiquitous families of chromatin-binding proteins. H1 molecules are involved in diverse nuclear processes, and their intranuclear organization is affected by various cellular conditions and stimuli (8,9). We now show that following migration cues, the mobility of histone H1 is decreased in correlation with increased level of the heterochromatin marker histone H3 lysine 9 tri-methylation (H3K9me3). Altered properties of linker histone in migrating nuclei are evolutionary conserved and were also found in the fungus *Neurospora crassa*. Furthermore, alterations in the interaction of H1 with chromatin altered the rate of cell migration. Our data suggest that cellular migration requires global changes in histones H1 and H3, which are associated with increased chromatin compaction.

Results and Discussion

Migration induction affects histone H1 organization

Histone H1 was chosen as a model chromatin component to examine whether early stages of cell migration involve global changes in the chromatin fibers. Migration was studied in the mouse melanoma cell line B16-F1 using the well-established wound healing assay (10). The cells were grown to confluence and scraped. As a result, the cells facing the wound sensed the lack of contact inhibition and migrated into the empty space. At fixed time-points after scraping, the cells were fixed and immunostained for histone H1 using either polyclonal antibodies (11) (Figure 1 A,D,G,J,M) or a monoclonal antibody AE4 (Figure 1 B,E,H,K,N), both were shown to be specific for H1. The immunostaining pattern using the H1 polyclonal antibodies did not vary amongst the studied time-points, suggesting that induction of migration does not alter the total amount or the intranuclear localization of H1. However, the immunostaining observed with the AE4 antibody suggested that external migration cues induce a dynamic response in the nuclear organization of H1. Within 30 min of migration

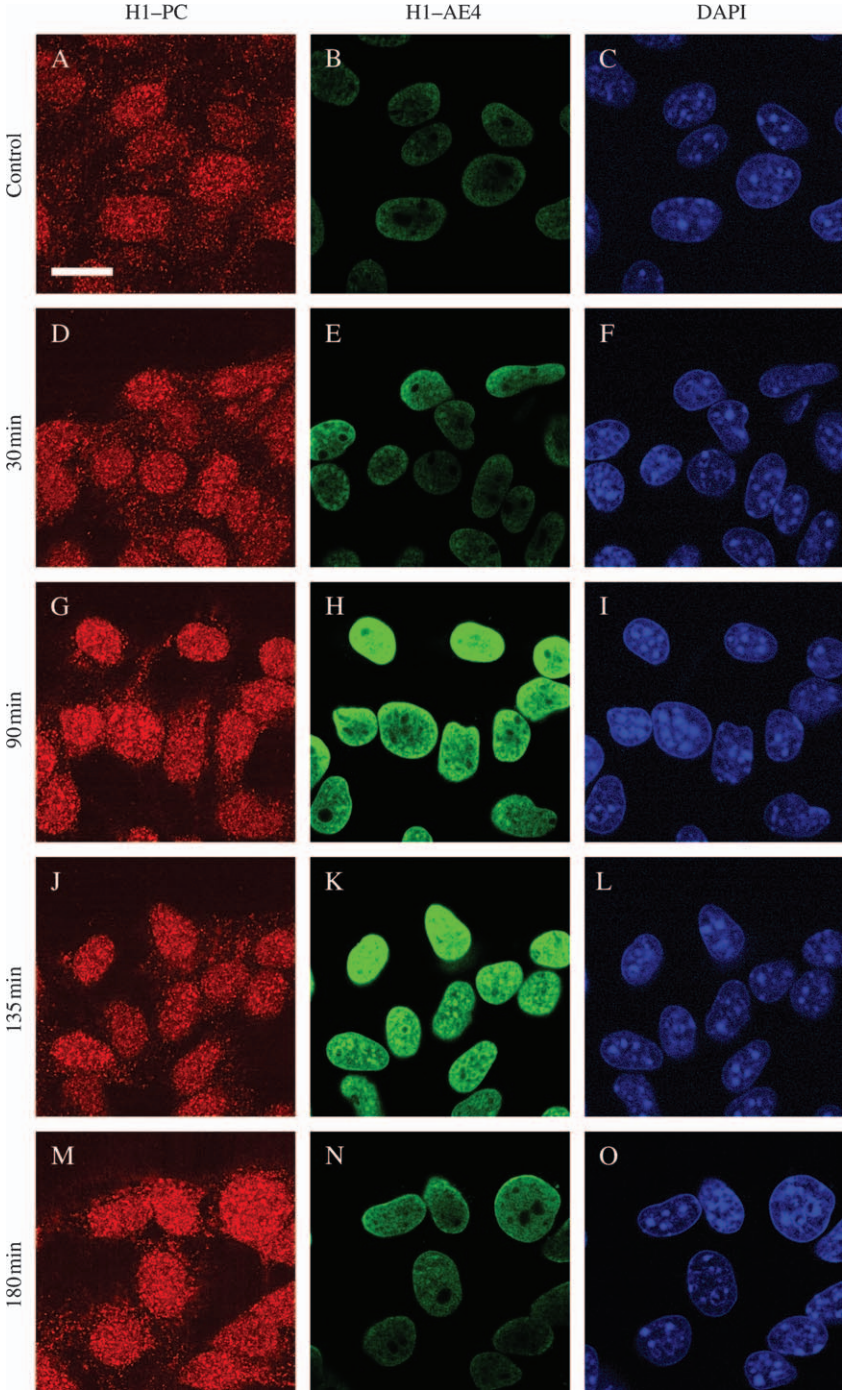

Figure 1: Altered H1 organization induced by directed cell migration. Shown are B16-F1 cells immunostained following a wound healing assay. A, D, G, J and M) Immunostaining with anti H1 polyclonal antibodies (H1–PC). B, E, H, K and N) Immunostaining with anti H1 monoclonal antibody AE4 (H1–AE4). C, F, I, L and O) DAPI staining. The time-points are shown on the left side of each row: A–C, control staining (prior to wound induction); D–F, 30 min; G–I, 90 min; J–L, 135 min; and M–O, 180 min. The wound edge is at the top of the pictures. The scale bar is 30 μm.

induction, the intensity of the AE4-specific immunostaining signal significantly increased in the cells positioned in close vicinity to the wound. The staining was further increased at the 90 min and 135 min time-points but decreased at the 180 min time-point, suggesting that the H1 changes are temporary and reversible. Interestingly, the nuclei were stained in a polarized manner; the cells closest to the wound stained most intensely. As the immunostaining of the total amount of H1 by the polyclonal antibodies was not altered, we concluded that most likely during the early stages of cell migration, a fraction of H1 is modified. One of the most common alterations in histone H1 is a reversible and transient phosphorylation, which can be inhibited by staurosporine and olomoucine (12,13). Interestingly, the presence of either of these two substances during the wound healing assay did not inhibit the transient increase in H1 immunostaining with the AE4 antibody (Figure 2). On the contrary, olomoucine treatment even further elevated the intensity of the migration-induced H1 immunostaining. As olomoucine is a cyclin dependent

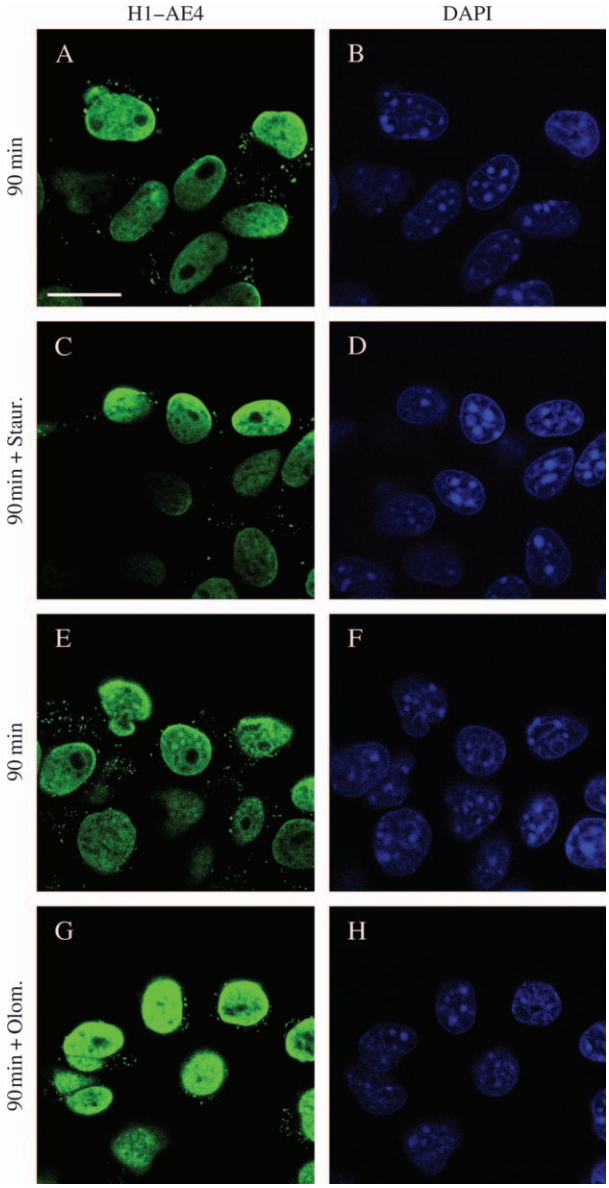

Figure 2: Protein kinase inhibitors increase the altered H1 organization induced by directed cell migration. A, C, E and G) Immunostaining with the mouse anti H1 monoclonal antibody AE4 (H1–AE4). B, D, F and H) DAPI staining. All points were immunostained 90 min following wound healing induction. Protein kinases inhibitors: C and D) 200 nM staurosporine. G and H) 300 μM olomoucine. The inhibitors were added 90 min before the introduction of the scratch. The wound edge is at the top of the pictures. The scale bar is 30 μm. Staur, staurosporine; Olom, olomoucine.

kinase (CDK) inhibitor, the results suggest that the altered immunostaining is because of H1 dephosphorylation. Previously, it was shown that the prevention of H1 phosphorylation on its CDK consensus phosphorylation sites decreases its mobility rate (14). Therefore, we hypothesized that the migration induction changes in immunostaining may be associated with reduced mobility of histone H1.

Migration induction leads to decreased mobility of histone H1

In order to evaluate the mobility properties of histone H1 in living cells, the H1E variant was cloned upstream to the green fluorescent protein (GFP). Evaluation of the fused protein reveled colocalization with Hoechst staining in live cells (Figure 3A–C), indicating typical H1 nuclear distribution (15,16). In addition, the GFP-fused protein was released from the nuclei by stepwise salt extraction similar to endogenous H1 (Figure 3D), indicating compatible chromatin-binding properties. Next, the dynamics of migration-induced changes in the binding of H1 to chromatin was determined by fluorescence recovery after photobleaching (FRAP) analysis, a technique suitable for determining the relative exchange rate of H1 molecules on chromatin in living cells in real time (15,16). Transfected H1E–GFP was photobleached within defined nuclear areas, and the recovery of the fluorescence within the photobleached areas was monitored. The rate of recovery is inversely proportional to the time that H1 histones reside on the chromatin (9), and therefore, increased H1 chromatin binding would lead to reduced movement of the protein and longer florescence recovery times. The H1E–GFP FRAP was monitored in confluent B16-F1 cells before and at fixed time-points after scratching. Measurements were taken in cells facing the scratch, and the time needed for 50% recovery (T_{50}) of the H1E–GFP pre-bleach fluorescence intensity was calculated and used for comparison between the different time-points (Figure 4). Interestingly, the H1E–GFP T_{50} increased 30 min and 90 min after migration induction by 50% and 70%, respectively, and returned to pre-scratch levels within 135 min (Figure 4B). The FRAP results indicate that in response to migration cues, histone H1 undergoes a temporary decrease in intranuclear mobility in a time frame which is similar to the changes observed by immunofluorescence (Figure 1). Collectively, the findings suggest that in migrating cells, H1 is temporarily dephosphorylated and therefore binds more tightly to the chromatin fiber.

Migration induction leads to increase in H3K9me3

Increased chromatin residence time of histone H1 is correlated with increased H3K9me3, a modification that is highly enriched in heterochromatin (17). This correlation was observed during early stages of embryogenesis (18) and during promoter closure (19). Moreover, heterochromatin-associated H1 has a lower mobility rate than euchromatin-associated H1 (16,20). Therefore, the reduced H1 mobility following migration induction led us to examine the dynamics of the heterochromatin marker, H3K9me3. Time-specific increase in immunostaining of H3K9me3 in the cells facing the wound was observed (Figure 5A,E,I, M,Q). Interestingly, immunostaining of histone H3 lysine 9 mono-methylation, a modification that is mostly excluded from mammalian heterochromatin (21,22) did not change in response to the migration cues (Figure 5C,G,K,O,S). The increase in levels of H3K9me3 was observed already

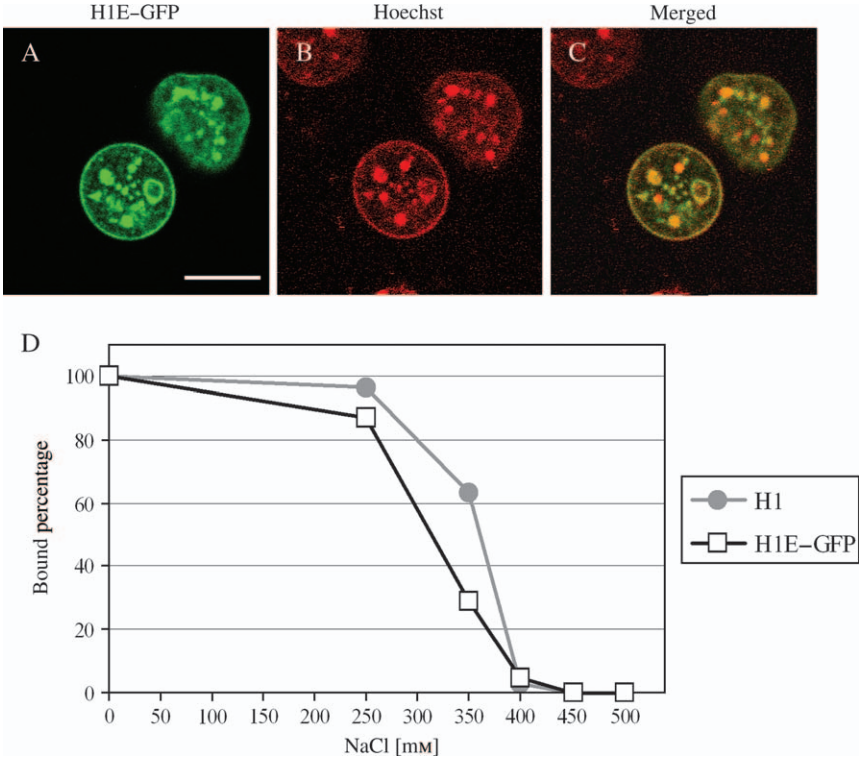

Figure 3: H1E–GFP properties are compatible with the properties of the endogenous histone H1. A, B and C) Localization of H1E–GFP in B16-F1 cells. Live B16-F1 cells overexpressing H1E–GFP were stained for DNA by Hoechst 33342. A, H1E–GFP; B, Hoechst; and C, merged panels A and B. The scale bar is 10 μm. D) Salt extraction properties of H1E–GFP and endogenous H1. H1 was extracted from B16-F1 cells overexpressing H1E–GFP using the indicated NaCl concentrations. Endogenous H1 and GFP-fusion proteins that were released into the supernatant or retained in the chromatin pellet were detected by Western blot analysis. The images were scanned, and the band intensities were quantified. The relative-retained fractions of endogenous (gray line) and exogenous H1 (black line) were calculated.

30 min after migration induction and continued throughout the time examined. Interestingly, the main increase in H3K9me3 was in the nuclear periphery, suggesting that the induction of directed cell migration leads to increased compaction of the chromatin next to the nuclear envelope.

Modulation of H1 chromatin-binding properties alters the rate of cell migration

These results suggested that alteration in H1–chromatin interaction is part of the mechanism that regulates directed cell migration. This possibility was examined using a new approach to lower the H1 chromatin-binding affinity. Previous studies demonstrated that the C-terminal domain of H1 binds weakly and non-specifically the linker DNA (23). Therefore, we reasoned that overexpression of the C-terminal domain of H1 will reduce the chromatin-binding affinity of the full-length endogenous H1. Cells were transfected with plasmids expressing either full-length H1E histone or an H1 deletion mutant containing only the 106 long lysine rich C-terminal half of the molecule, both fused to GFP. The chromatin-binding affinity of the endogenous H1 in the transfected cells was monitored by stepwise salt extraction. As shown in Figure 6A, small amounts (~5%) of endogenous H1 were released from nuclei overexpressing the H1 C-terminal domain at NaCl concentrations of 0–150 mM, whereas no endogenous H1 was released from nuclei overexpressing full-length H1. Interestingly, at 250 mM NaCl, still no endogenous H1 was released from full-length H1 overexpressing nuclei, while one third of the endogenous H1 was released from nuclei overexpressing the H1 C-terminal domain. Thus, the C-terminal domain of histone H1 can be used as a tool to reduce H1 chromatin-binding affinity. To test our hypothesis that the binding of H1 to chromatin plays a role in cell migration, two assays were used; the Transwell and the wound healing assays. The migration rates of cells overexpressing H1E C-terminal domain were compared with that of the control cells. In the Transwell assay, transfected cells were plated on top of filters, and their migration rate through fibronectin-coated pores toward the lower part of the filter was measured. Overexpression of the C-terminal domain of H1E inhibited cell migration by 34% in comparison to overexpression of the GFP (Figure 6B). In the wound healing assay, the same fields of confluent transfected cells were pictured right after the scratch (time 0) as well as 11 h of incubation following the scratch time. The area covered by the migrated cells was measured, and their relative migration rate was calculated (Figure 6C,D). Interestingly, overexpression of the C-terminal domain of H1E accelerated the rate of cell migration by 2.5-fold in comparison to overexpression of the GFP protein. The reverse effects of H1E C-terminal domain overexpression on cell migration rate as measured by the Transwell assay and the wound healing assay may be because of the different migration mechanism used in these two assays. In the Transwell assay, the cells use more amoeboid-like movements (24,25) and are probably required for significant morphological changes in the nuclear shape in order to pass through pores that are smaller than their normal cell width. In the wound healing assay, the cells use mesenchymal-like-polarized motility (24,25), which probably

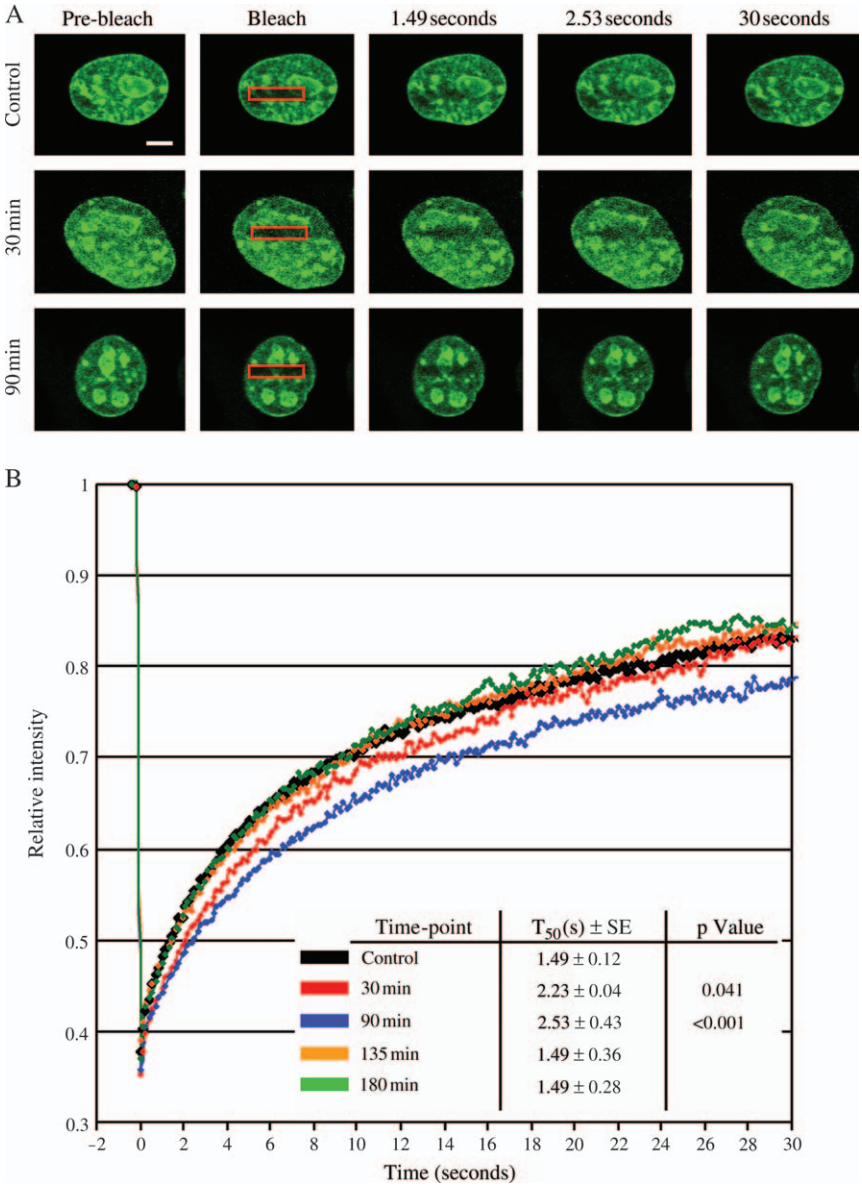

Figure 4: Induction of cell migration alters the mobility of H1. Shown are FRAP analyses of H1E–GFP overexpressed in B16-F1 cells during a wound healing assay. A) Representative images of cells facing the wound edge before and after photobleaching of the marked area (red rectangular) at the indicated time-points. The scale bar is 5 μm. B) Quantitative FRAP analysis of the results. The average time required for 50% recovery of the fluorescence of the bleached area ±standard error (SE) from 8 to 10 cells in each time-point is presented. The statistical significance relative to the control was determined by the Student's *t*-test.

requires less changes in the nuclear shape. Such opposite effects of overexpressed protein on cell migration have been also found in studies on the migration regulatory effects of the $p27^{kip1}$ protein. Overexpression of $p27^{kip1}$ inhibited cell migration in Transwell assays (26–28), while accelerated migration in wound healing assays (29,30). Nonetheless, these significant effects of the C-terminal domain of H1E on the rate of cell migration suggest that changes in the binding properties of H1 to chromatin are involved in regulation of cell migration.

H1 reorganization is not confined to mammalian cells

As nuclear migration is a fundamental event in all eukaryotes (31), we searched for another example in which reorganization of chromatin occurs in response to migration cues, and nuclear motility is easily observable. In a study in *N. crassa* where histone H1 was tagged with GFP, dynamic nuclear speckles were noted (32). We re-examined this strain at several time-points following spore germination (1, 2, 5 and 6.5 h). The analysis indicated that following spore germination, within the newly formed short hyphae (200–1000 μm), nuclei are highly motile. We examined the nuclear organization of H1 in the motile nuclei by taking a movie of the living cells 6.5 h after spore germination (representative pictures are shown in Figure 7 and Movie S1). Interestingly, a bright signal of accumulated H1–GFP always appeared in the leading edge of the motile nuclei. These results suggest that histone H1 reorganization in response to migration cues is an evolutionary conserved trait.

In conclusion, our results indicate that induction of directed cell migration leads to global changes in chromatin organization. In mouse B16-F1 cells, these changes involve

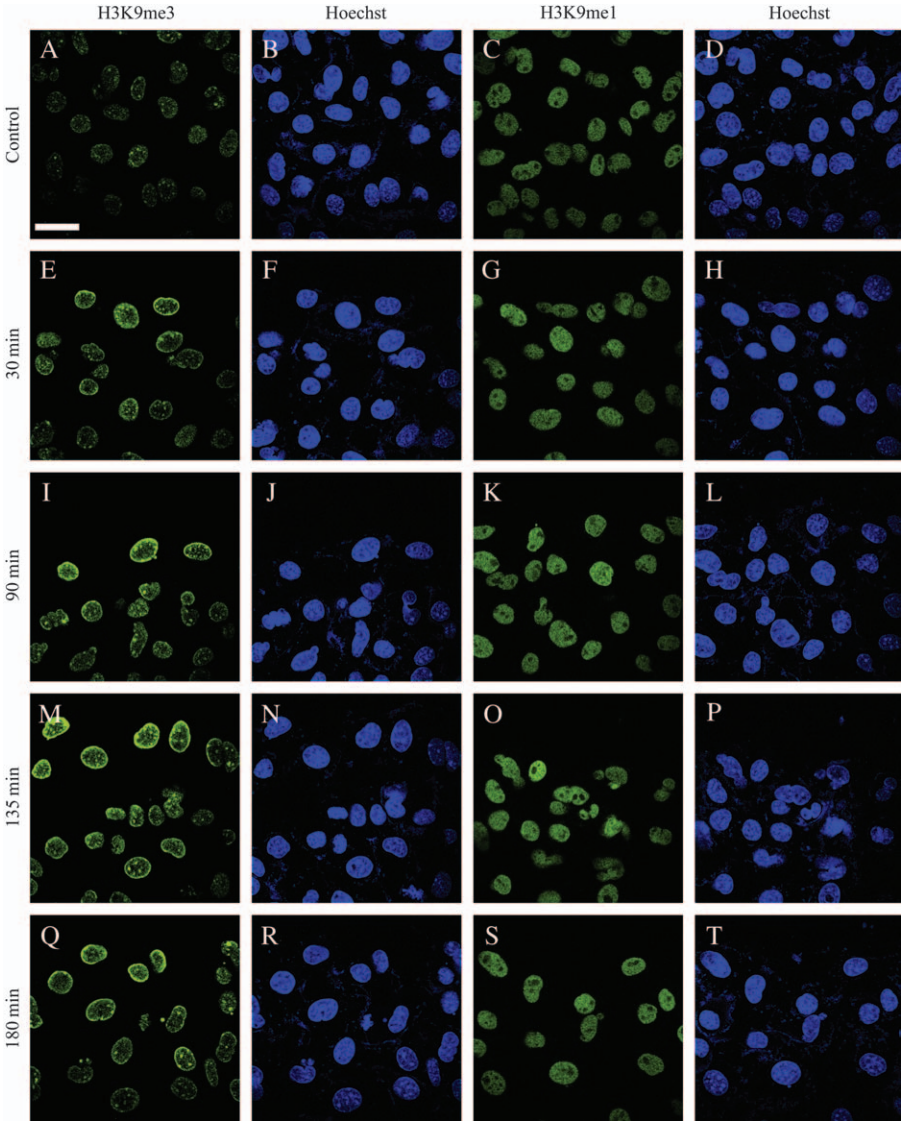

Figure 5: Induction of cell migration elevates the levels of H3K9me3. Shown are B16-F1 cells immunostained following a wound healing assay. A, E, I, M and Q) Immunostaining with antibodies against H3K9me3. C, G, K, O and S) Immunostaining with antibodies against histone H3 lysine 9 monomethylation (H3K9me1). B, D, F, H, J, L, N, P, R and T) Hoechst staining. The time-points are shown on the left side of each row: A–D, control staining (prior to wound induction); E–H, 30 min; I–L, 90 min; M–P, 135 min; and Q–T, 180 min. The wound edge is at the top of the pictures. The scale bar is 50 μm.

a transient increase in the chromatin binding of histone H1 along with an elevation in the heterochromatin marker H3K9me3. In migrating nuclei of fungi, relocalization of H1 was observed. H1 is the most abundant structural nucleosome-binding protein, thus chosen as the focus of our studies. In the living nucleus, H1 functions within a dynamic network of chromatin-binding proteins that continuously compete for chromatin-binding sites (9). This network includes members of the high-mobility group protein superfamily (33) and perhaps, other proteins such as the HP1, Polycomb group and methyl-cytosine–phosphate–guanosine-binding domain proteins. Histone H1 and some other members of this protein network preferentially bind to heterochromatin, and their binding apparently increases following induction of directed cell migration. Thus, the possible reorganization of other chromatin-binding proteins during cellular migration is likely. Furthermore, increased heterochromatin formation is often associated with transcriptional repression (17,34), which can occur in response to migration cues. The major increase in peripheral heterochromatin level and H1 chromatin binding in response to migration cues along with previous results showing direct interaction between heterochromatin, histone H1 and nuclear envelope proteins (35–37) may indicate increased anchoring of the chromatin fiber to the nuclear envelope upon migration induction. Our study indicates that cellular migration induces and is contingent on global changes in chromatin organization. So far, very little is known about the role of chromatin in cell migration; obviously, this complex process requires further investigation.

Materials and Methods

Plasmids

The human H1E originated from the IMAGE clone 6498952 (Invitrogen Life Technologies). The ORF was released using *Eco*RI and *Eco*RV restriction enzymes and inserted into pBluescript II KS+ (Stratagene) to generate

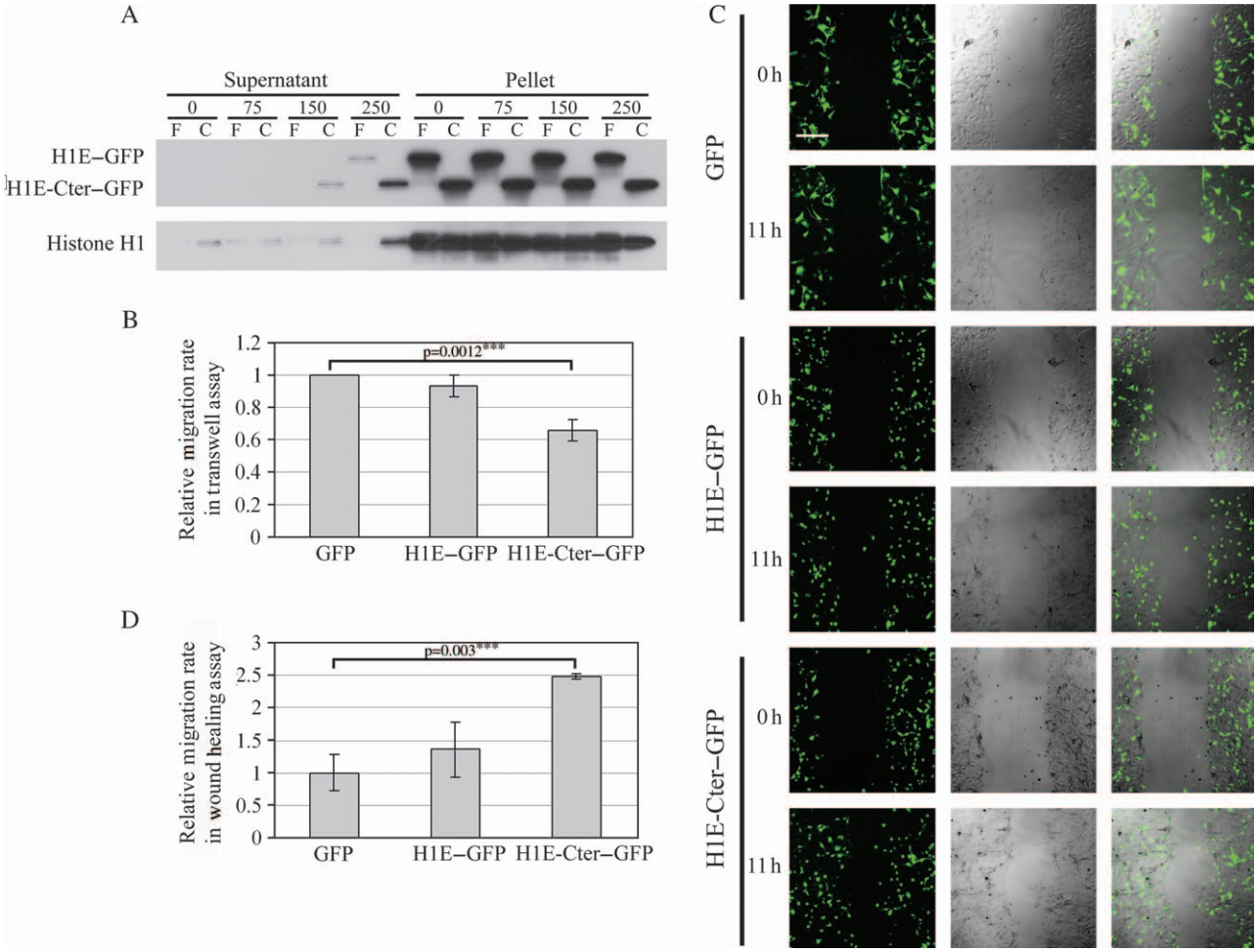

Figure 6: The C-terminal domain of histone H1 decreases the chromatin binding of endogenous H1 and alters the rate of cell migration. A) H1 was extracted from 293 cells overexpressing full-length H1E fused to GFP (F) or C-terminal domain of H1E fused to GFP (C) using the NaCl concentrations shown on top of the columns (values represent concentrations in mM). The endogenous H1 and the GFP-fusion proteins that were released into the supernatant or retained in the chromatin pellet were detected by Western blot analysis. B) Overexpression of H1E C-terminal domain inhibits cell migration in Transwell assay. Migration rates of B16-F1 overexpressing either GFP or histone H1E fused to GFP or C-terminal part of H1E fused to GFP were measured by the Transwell assay. Three hours following plating the cells on top of fibronectin precoated membranes, the cells were fixed in paraformaldehyde and counted on both sides of the membranes. In each experiment, the average number of migrated cells was divided by the average total number of cells, and the ratio in the GFP-transfected cells was set as one. The represented results are an average of four repetitions ±standard error. The statistical significance relative to the control was determined by the Student's *t*-test. C) Overexpression of H1E C-terminal domain accelerates cell migration in a wound healing assay. The migration rate of B16-F1 overexpressing either GFP or histone H1E fused to GFP or C-terminal part of H1E fused to GFP was measured by the wound healing assay. Shown are representative pictures of GFP, phase contrast and merged pictures of the same fields right after the scratch, time 0 and 11 h later. The scale bar is 200 μm. D) The area covered by the cells after 11 h of incubation was measured and was set as one in the GFP-transfected cells. The represented results are an average of three repetitions ±standard error. The statistical significance relative to the control was determined by the Student's *t*-test.

pBS–H1E. Following sequencing, an insertion mutation at position 575 of the IMAGE clone was corrected by polymerase chain reaction (PCR) using oligonucleotides hH1E3 (5′-cagaattcaacatgtccgagactgcg-3′) and hH1E6 (5′-cttttcgctttttttggctccagcagctgc-3′) to amplify nucleotides 1–525 of H1E ORF and hH1E4 (5′-ctctcgagcttttttcttggctgccgcct-3′) and hH1E5 (5′-ggagc-caaaaaagcgaaaagcccgaaaaag-3′) and to amplify nucleotides 496–717 of H1E ORF. The two generated fragments were mixed and amplified by oligonucleotides hH1E3 and hH1E6 to generate the correct H1E ORF, which was inserted into *Eco*RI–*Xho*I sites of pcDNA3 (Invitrogen) to generate pcH1E. The H1E ORF as an *Eco*RI-filled-*Xho*I fragment from pcH1E was placed upstream to GFP using the *Eco*47III–*Xho*I sites in pEGFP–N1 (Clontech) to generate pH1E–GFP. The C-terminal part of H1E (aa 113–218) was amplified by PCR using oligonucleotides hH1E9 (5′-cgctagccatgtctggggaagccaagcctaa-3′) and hH1E4 and inserted upstream to GFP using *Nhe*I–*Xho*I sites in pEGFP–N1 to generate pCter-H1E–GFP.

Cell culture and immunostaining

Mouse melanoma B16-F1 and human HEK293 cell lines were grown as described (38,39). B16-F1 cells plated on fibronectin-coated cover slides (F4759; Sigma) and grown to confluence were scratched for wound healing assay. Where indicated 300 μM olomoucine (#495620; Calbiochem) or 200 nM staurosporine (#569397; Calbiochem) were added 90 min prior to the wound healing assay. Following further incubation at growth conditions,

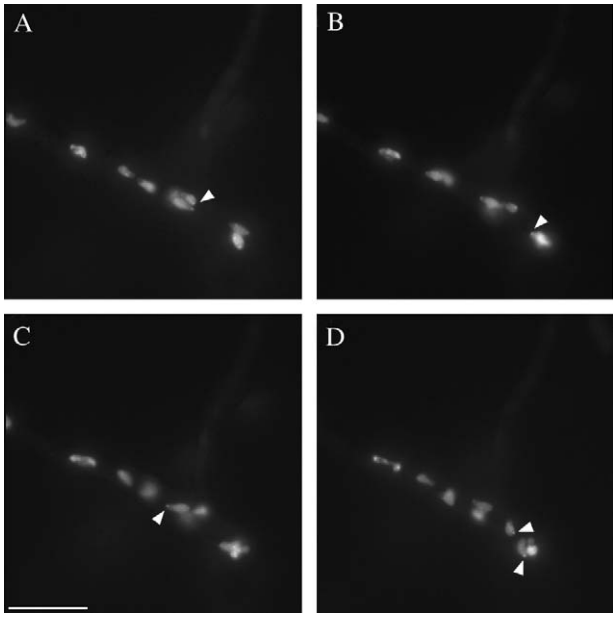

Figure 7: Histone H1 is preferentially concentrated in the leading edge of motile *N. crassa* nuclei. Pictures of germinating spores were taken every 2 seconds for 3 min. Representative pictures of 12, 62, 98 and 158 seconds time-points are shown in A–D, respectively. Scale bar size is 5 μm. The leading edges of the motile nuclei were identified in Movie S1, and arrows were drawn to mark accumulation of H1–GFP in the leading edge of the motile nuclei.

immunostaining was carried out as described (39). Antibodies included histone H1 antibodies: rabbit polyclonal (11) and AE4 monoclonal which was raised against nuclei from human myeloid leukemia cells (#8030; Santa-Cruz Biotechnology, Inc.), anti-tri-methyl histone H3 (Lys 9) rabbit polyclonal (#07-442; Upstate) and anti-mono-methyl histone H3 (Lys 9) rabbit polyclonal (#07-450; Upstate). Pictures of H1 were collected using a Bio-Rad Radiance 2100 confocal system mounted on a Nikon TE300 microscope. Pictures of H3 were collected using a Zeiss LSM 510 confocal microscope.

Fluorescence recovery after photobleaching

B16-F1 cells were transfected with pH1E–GFP using Lipofectamine™ 2000 (Invitrogen Life Technologies) 16 h prior to FRAP analysis with a Zeiss LSM 510 confocal microscope. Two pre-bleach images were collected, and a rectangular (11 × 2 μm) image was bleached by five pulses during 0.063 seconds. Single images were collected in 0.149-second intervals. The imaging laser, 488 nm laser, was set on 2% power, while the bleaching lasers, 458, 488, 514, 543 and 683 nm lasers, were set on 100% power. The fluorescence intensity in the bleached area was normalized to the initial fluorescence and to the total fluorescence reduction in the unbleached areas. Eight to eleven cells were analyzed in each time-point during 20 min. The experiment was repeated three times, and statistical analysis was determined using the Student's *t*-test.

Migration rate assays

For Transwell assay, B16-F1 cells were transfected with pGFP or pH1E–GFP or pCter-H1E–GFP using JetPEI™ (PolyPlus; Illkirch Cedex). Forty-eight hours later, the lower sides of Transwell® plate (#3422; Costar) filters were precoated with 0.01 mg/mL of fibronectin. The filters were placed in the lower chambers containing 600 μL DMEM and 1.5×10^5 cells in 100 μL of DMEM were added to the upper chambers, followed with 3-h incubation at growth conditions. Membranes were fixed for 20 min in 3% paraformaldehyde–PBS, washed three times in PBS and cut off their holders. Transfected cells on each membrane side were counted under a ×20 objective. Six membranes were used for each point, of which three were used for counting the non-migrated cells in the upper side (three different fields in each membrane) and three for counting the migrated cells in the lower side (six different fields in each membrane because of the lower number of cells). In each experiment, the average number of migrated cells was divided by the average total number of cells, and the ratio in the GFP-transfected cells was set as one. The represented results are an average of four repetitions, and statistical significance was determined using the Student's *t*-test.

For wound healing assay, B16-F1 cells plated on fibronectin-coated plates were grown to confluence and were transfected with GFP or pH1E–GFP or pCter-H1E–GFP using Lipofectamine™ 2000 (Invitrogen Life Technologies). Twenty-four hours later, the cells were washed three times with PBS, scratched with white tip and kept in medium containing 0.1% fetal calf serum for 11 h. Pictures were collected using a Zeiss LSM 510 confocal microscope right after the scratch and at the end of the incubation time. The covered area by the migrating cells was measured by the ImageJ 1.37V program. The covered area in the GFP-transfected cells was set as one. The represented results are an average of three repetitions, and statistical significance was determined using the Student's *t*-test.

Stepwise salt extraction

HEK293 or B16-F1 cells were transfected with pH1E–GFP or pCter-H1E–GFP. Following 48 h, the cells were collected and washed twice with PBS and three times with buffer I [20 mM K-HEPES, pH 7.6; 10 mM KCl; 10 mM $MgCl_2$; 20% glycerol; 0.1% Triton-X-100; 25 mM NaF; 10 mM β-glycerolphosphate; 1 mM Na-Vandate; and 0.5 mM DTT supplemented with protease inhibitors (P8340; Sigma)]. Resuspension of the cells in buffer I supplemented with various NaCl concentrations was followed by 15-min incubation on ice and 5 min centrifugation at 7800× ***g***. The supernatants were separated from the nuclei pellets, which were lysed by sonication in SDS sample buffer. Equal cell amounts were analyzed by Western blot analysis using rabbit polyclonal antibodies against histone H1 and mouse monoclonal antibodies against GFP (#1814460; Roche).

Neurospora crassa *assays*

Neurospora crassa strain N2282A (*his-3*$^+$*::Pccg-1-hH1*$^+$*-sgfp*$^+$) kindly provided by M. Freitag (32) was used. Procedures used were as described (40). For germination experiments, 2×10^5 spores/mL were inoculated and grown for 2–6.5 h at 34°C, 150 rpm. Germinating spores were taken for time-lapse microscopy using the Applied-imaging system. One milliliter of the suspension was placed on a glass-bottom tissue culture plate (#P35GC-1.5-14-C; MatTek Corporation).

Acknowledgments

We would like to thank Susan H. Garfield and Stephen M. Wincovitch (LEC, CCR, NCI) for their help with the confocal microscopy. The work has been supported by the Israeli Science Foundation (grants number 270/04 to O. R. and 556/04 to O. Y.), the Foundation Jérôme Lejeune, the Minerva foundation, the Federal German Ministry for Education and Research, the Israeli Cancer Association, the German–Israeli collaboration grant Gr-1905, the David and Fela Shapell Family Center for Genetic Disorders Research and by the Intramural Research Program of the National Institutes of Health, Center for Cancer Research, National Cancer Institute. O. R. is an incumbent of the Berstein-Mason professorial chair of Neurochemistry.

Supplementary Material

Movie S1: *Neurospora crassa* time-lapse microscopy. Following germination, GFP H1 histone nuclei were followed using time-lapse microscopy as described in the *Materials and Methods*.

Supplemental materials are available as part of the online article at http://www.blackwell-synergy.com

References

1. Ridley AJ, Schwartz MA, Burridge K, Firtel RA, Ginsberg MH, Borisy G, Parsons JT, Horwitz AR. Cell migration: integrating signals from front to back. Science 2003;302:1704–1709.
2. Vicente-Manzanares M, Webb DJ, Horwitz AR. Cell migration at a glance. J Cell Sci 2005;118:4917–4919.
3. Gomes ER, Jani S, Gundersen GG. Nuclear movement regulated by Cdc42, MRCK, myosin, and actin flow establishes MTOC polarization in migrating cells. Cell 2005;121:451–463.
4. Colon-Ramos DA, Salisbury JL, Sanders MA, Shenoy SM, Singer RH, Garcia-Blanco MA. Asymmetric distribution of nuclear pore complexes and the cytoplasmic localization of beta2-tubulin mRNA in Chlamydomonas reinhardtii. Dev Cell 2003;4:941–952.
5. Yamauchi K, Yang M, Jiang P, Yamamoto N, Xu M, Amoh Y, Tsuji K, Bouvet M, Tsuchiya H, Tomita K, Moossa AR, Hoffman RM. Real-time in vivo dual-color imaging of intracapillary cancer cell and nucleus deformation and migration. Cancer Res 2005;65:4246–4252.
6. Bellion A, Baudoin JP, Alvarez C, Bornens M, Metin C. Nucleokinesis in tangentially migrating neurons comprises two alternating phases: forward migration of the Golgi/centrosome associated with centrosome splitting and myosin contraction at the rear. J Neurosci 2005; 25:5691–5699.
7. Schaar BT, McConnell SK. Cytoskeletal coordination during neuronal migration. Proc Natl Acad Sci U S A 2005;102:13652–13657.
8. Bustin M, Catez F, Lim JH. The dynamics of histone H1 function in chromatin. Mol Cell 2005;17:617–620.
9. Catez F, Ueda T, Bustin M. Determinants of histone H1 mobility and chromatin binding in living cells. Nat Struct Mol Biol 2006;13: 305–310.
10. Valster A, Tran NL, Nakada M, Berens ME, Chan AY, Symons M. Cell migration and invasion assays. Methods 2005;37:208–215.
11. Bustin M, Stollar BD. Immunological relatedness of thymus and liver F1 histone subfractions. J Biol Chem 1973;248:3506–3510.
12. Banks GC, Deterding LJ, Tomer KB, Archer TK. Hormone-mediated dephosphorylation of specific histone H1 isoforms. J Biol Chem 2001; 276:36467–36473.
13. Paulson JR, Patzlaff JS, Vallis AJ. Evidence that the endogenous histone H1 phosphatase in HeLa mitotic chromosomes is protein phosphatase 1, not protein phosphatase 2A. J Cell Sci 1996;109:1437–1447.
14. Contreras A, Hale TK, Stenoien DL, Rosen JM, Mancini MA, Herrera RE. The dynamic mobility of histone H1 is regulated by cyclin/CDK phosphorylation. Mol Cell Biol 2003;23:8626–8636.
15. Lever MA, Th'ng JP, Sun X, Hendzel MJ. Rapid exchange of histone H1.1 on chromatin in living human cells. Nature 2000;408:873–876.
16. Misteli T, Gunjan A, Hock R, Bustin M, Brown DT. Dynamic binding of histone H1 to chromatin in living cells. Nature 2000;408:877–881.
17. Grewal SI, Jia S. Heterochromatin revisited. Nat Rev Genet 2007;8:35–46.
18. Meshorer E, Yellajoshula D, George E, Scambler PJ, Brown DT, Misteli T. Hyperdynamic plasticity of chromatin proteins in pluripotent embryonic stem cells. Dev Cell 2006;10:105–116.
19. Vaquero A, Scher M, Lee D, Erdjument-Bromage H, Tempst P, Reinberg D. Human SirT1 interacts with histone H1 and promotes formation of facultative heterochromatin. Mol Cell 2004;16:93–105.
20. Catez F, Brown DT, Misteli T, Bustin M. Competition between histone H1 and HMGN proteins for chromatin binding sites. EMBO Rep 2002; 3:760–766.
21. Peters AH, Kubicek S, Mechtler K, O'Sullivan RJ, Derijck AA, Perez-Burgos L, Kohlmaier A, Opravil S, Tachibana M, Shinkai Y, Martens JH, Jenuwein T. Partitioning and plasticity of repressive histone methylation states in mammalian chromatin. Mol Cell 2003;12:1577–1589.
22. Rice JC, Briggs SD, Ueberheide B, Barber CM, Shabanowitz J, Hunt DF, Shinkai Y, Allis CD. Histone methyltransferases direct different degrees of methylation to define distinct chromatin domains. Mol Cell 2003; 12:1591–1598.
23. Brown DT, Izard T, Misteli T. Mapping the interaction surface of linker histone H1(0) with the nucleosome of native chromatin in vivo. Nat Struct Mol Biol 2006;13:250–255.
24. Friedl P, Wolf K. Tumour-cell invasion and migration: diversity and escape mechanisms. Nat Rev Cancer 2003;3:362–374.
25. Webb DJ, Horwitz AF. New dimensions in cell migration. Nat Cell Biol 2003;5:690–692.
26. Baldassarre G, Belletti B, Nicoloso MS, Schiappacassi M, Vecchione A, Spessotto P, Morrione A, Canzonieri V, Colombatti A. p27(Kip1)-stathmin interaction influences sarcoma cell migration and invasion. Cancer Cell 2005;7:51–63.
27. Daniel C, Pippin J, Shankland SJ, Hugo C. The rapamycin derivative RAD inhibits mesangial cell migration through the CDK-inhibitor p27KIP1. Lab Invest 2004;84:588–596.
28. Sun J, Marx SO, Chen HJ, Poon M, Marks AR, Rabbani LE. Role for p27(Kip1) in vascular smooth muscle cell migration. Circulation 2001; 103:2967–2972.
29. Besson A, Gurian-West M, Schmidt A, Hall A, Roberts JM. p27Kip1 modulates cell migration through the regulation of RhoA activation. Genes Dev 2004;18:862–876.
30. McAllister SS, Becker-Hapak M, Pintucci G, Pagano M, Dowdy SF. Novel p27(kip1) C-terminal scatter domain mediates Rac-dependent cell migration independent of cell cycle arrest functions. Mol Cell Biol 2003;23:216–228.
31. Morris NR. Nuclear migration. From fungi to the mammalian brain. J Cell Biol 2000;148:1097–1101.
32. Freitag M, Hickey PC, Raju NB, Selker EU, Read ND. GFP as a tool to analyze the organization, dynamics and function of nuclei and microtubules in *Neurospora crassa*. Fungal Genet Biol 2004;41:897–910.
33. Catez F, Yang H, Tracey KJ, Reeves R, Misteli T, Bustin M. Network of dynamic interactions between histone H1 and high-mobility-group proteins in chromatin. Mol Cell Biol 2004;24:4321–4328.
34. Craig JM. Heterochromatin – many flavours, common themes. Bioessays 2005;27:17–28.
35. Makatsori D, Kourmouli N, Polioudaki H, Shultz LD, McLean K, Theodoropoulos PA, Singh PB, Georgatos SD. The inner nuclear membrane protein lamin B receptor forms distinct microdomains and links epigenetically marked chromatin to the nuclear envelope. J Biol Chem 2004;279:25567–25573.
36. Montes de Oca R, Lee KK, Wilson KL. Binding of barrier to autointegration factor (BAF) to histone H3 and selected linker histones including H1.1. J Biol Chem 2005;280:42252–42262.
37. Ye Q, Worman HJ. Interaction between an integral protein of the nuclear envelope inner membrane and human chromodomain proteins homologous to Drosophila HP1. J Biol Chem 1996;271:14653–14656.
38. Porgador A, Feldman M, Eisenbach L. H-2Kb transfection of B16 melanoma cells results in reduced tumourigenicity and metastatic competence. J Immunogenet 1989;16:291–303.
39. Gerlitz G, Darhin E, Giorgio G, Franco B, Reiner O. Novel functional features of the Lis-H domain: role in protein dimerization, half-life and cellular localization. Cell Cycle 2005;4:1632–1640.
40. Davis RH. Neurospora: Contributions of a Model Organism. Oxford: Oxford University Press; 2000.